

Differential Surface Adsorption Phenomena for Conventional and Novel Surfactants Correlates with Changes in Interfacial mAb Stabilization

Ankit D. Kanthe,* Miriam R. Carnovale, Joshua S. Katz, Susan Jordan, Mary E. Krause, Songyan Zheng, Andrew Ilott, William Ying, Wei Bu, Mrinal K. Bera, Binhua Lin, Charles Maldarelli, and Raymond S. Tu*

Cite This: *Mol. Pharmaceutics* 2022, 19, 3100–3113

Read Online

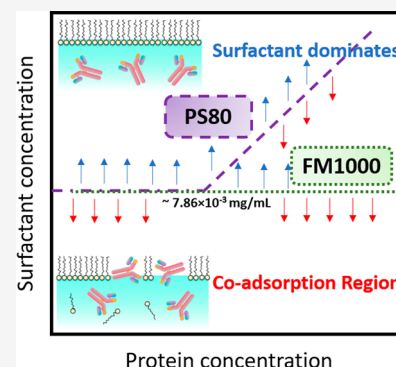
ACCESS |

Metrics & More

Article Recommendations

Supporting Information

ABSTRACT: Protein adsorption on surfaces can result in loss of drug product stability and efficacy during the production, storage, and administration of protein-based therapeutics. Surface-active agents (excipients) are typically added in protein formulations to prevent undesired interactions of proteins on surfaces and protein particle formation/aggregation in solution. The objective of this work is to understand the molecular-level competitive adsorption mechanism between the monoclonal antibody (mAb) and a commercially used excipient, polysorbate 80 (PS80), and a novel excipient, *N*-myristoyl phenylalanine-*N*-polyetheramine diamide (FM1000). The relative rate of adsorption of PS80 and FM1000 was studied by pendant bubble tensiometry. We find that FM1000 saturates the interface faster than PS80. Additionally, the surface-adsorbed amounts from X-ray reflectivity (XRR) measurements show that FM1000 blocks a larger percentage of interfacial area than PS80, indicating that a lower bulk FM1000 surface concentration is sufficient to prevent protein adsorption onto the air/water interface. XRR models reveal that with an increase in mAb concentration (0.5–2.5 mg/mL: IV based formulations), an increased amount of PS80 concentration (below critical micelle concentration, CMC) is required, whereas a fixed value of FM1000 concentration (above its relatively lower CMC) is sufficient to inhibit mAb adsorption, preventing mAb from co-existing with surfactants on the surface layer. With this observation, we show that the CMC of the surfactant is not the critical factor to indicate its ability to inhibit protein adsorption, especially for chemically different surfactants, PS80 and FM1000. Additionally, interface-induced aggregation studies indicate that at minimum surfactant concentration levels in protein formulations, fewer protein particles form in the presence of FM1000. Our results provide a mechanistic link between the adsorption of mAbs at the air/water interface and the aggregation induced by agitation in the presence of surfactants.



KEYWORDS: novel surfactants, protein formulations, protein aggregation, polysorbate 80 (PS80), FM1000, monoclonal antibody (mAb), X-ray reflectivity, pendant bubble tensiometry, surface tension, air/water interface, silicone oil/liquid interface

INTRODUCTION

Protein therapeutics such as monoclonal antibodies (mAbs) have become leading candidates for the treatment of autoimmune diseases, human cancer, and infectious diseases, among other indications.^{1,2} Due to mAbs' amphiphilic nature, adsorption of proteins from aqueous bulk solution onto surfaces (air/water, solid/liquid, or oil/water) has recently gained interest in the literature.^{3–13} Protein molecules are exposed to several interfaces during the manufacturing of the drug substance, processing of the drug product, and transportation, storage, and clinical administration. It has been hypothesized that as proteins adsorb onto surfaces, they can denature, unfold, and aggregate at interfaces, leading to protein particulates and aggregates in the bulk solution.^{14–16} Aggregates, sub-visible particles, and visible particles are detrimental to a biologic drug product as they can limit

product shelf-life, reduce the effective dose of the drug, and potentially implicate an immunological response.^{17–19} In order to enhance protein stability, protein formulations often containing excipients such as sugars,^{20,21} salts,^{22,23} and/or buffers^{20,24,25} and surfactants^{26–30} are employed to minimize the undesired interaction of proteins with surfaces.

The primary goal of this study was to compare two excipients' abilities to stabilize protein molecules in their native form by preventing unwanted surface adsorption and

Received: February 26, 2022

Revised: June 20, 2022

Accepted: June 21, 2022

Published: July 26, 2022



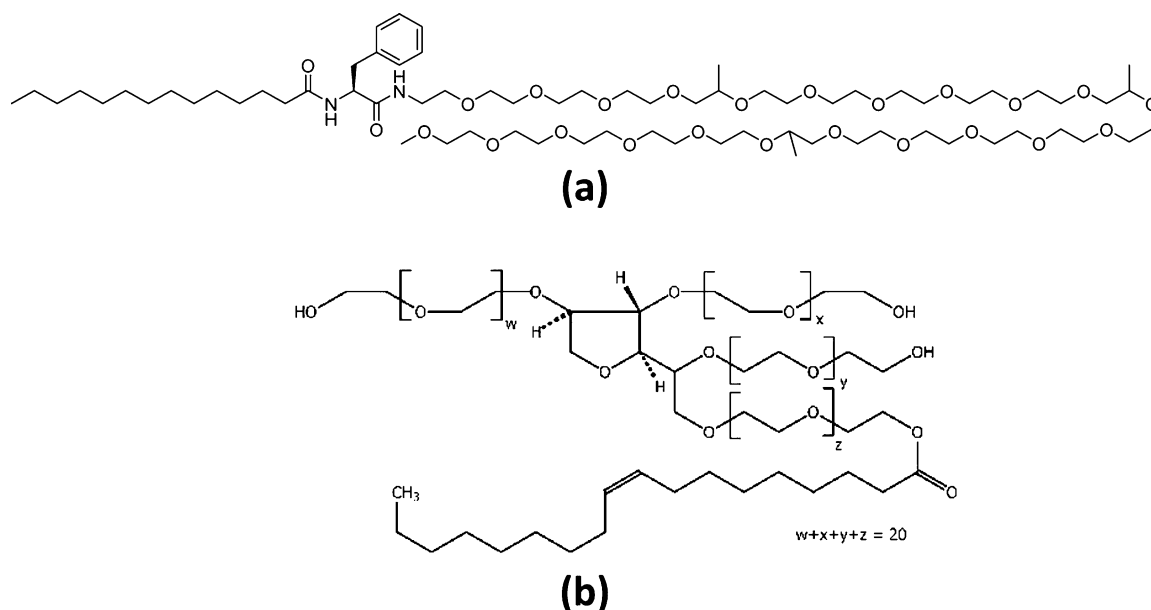


Figure 1. Molecular structure of surfactants (a) FM1000 and (b) PS80.

aggregation. There are currently two mechanistic pictures of how surfactants inhibit protein adsorption at the air/water interface. First, surfactants, being more surface active than proteins, can block the adsorption of proteins onto the surface, providing interfacial protection. Second, surfactants can interact with protein solutions in the bulk to protect regions prone to protein–protein interactions resulting in denaturation, although this mechanism is considered to be less dominant.^{29,31} As surfactants can prevent hydrophobically driven protein adsorption, there is a need to quantify the amount of surfactant in drug product formulation necessary to preserve the efficacy and shelf-life of therapeutic proteins. At sufficiently high protein concentrations, protein molecules can outcompete surfactants for the interface, resulting in a co-adsorbed film on surfaces due to competitive adsorption.

Polysorbates have been widely used in biologic drug products to stabilize protein formulations as they are considered safe. However, several stability challenges of polysorbates have been recently described in the literature.³² Degradation of polysorbates due to cleavage of the ester bond, resulting in the formation of free fatty acids over time, has been a subject of concern. Polysorbate degradation is known to occur through enzymatic hydrolysis or oxidation of polysorbates, resulting in decreased levels of free polysorbate monomers in the bulk solution.^{33–35} These fatty acids are insoluble and can form visible and sub-visible particles during the storage of protein drug products. Reduced concentrations of polysorbate due to degradation can be detrimental for the final drug product, affecting protection of mAbs from interfacial stress.^{34,36–40} Therefore, there is a need to explore alternative surfactants that can also inhibit protein adsorption. Poloxamer 188 (P188), a triblock copolymer consisting of repeating units of polyethylene oxide (PEO) and polypropylene oxide (PPO), is often used as an alternative surfactant to polysorbates.⁴¹ The absence of the ester bond in P188 makes it less susceptible to enzymatic degradation. On the other hand, the presence of hydrophilic polyether groups in P188 makes it more prone to oxidation. However, suppliers now provide poloxamer with a small amount of the inhibitor such as butylhydroxytoluene to prevent oxidation.⁴² Additionally, it

should be noted that current practices for incorporating surfactants in biologic formulations are mostly limited to polysorbates due to their long history of safe use. A more knowledge-driven approach to surfactant selection and optimization will be required to successfully advance the ever-expanding diversity of novel modalities such as cell and gene therapeutics, recent messenger RNA-based COVID-19 vaccines, recombinant adeno-associated viruses, antibody-drug conjugates, bispecific antibodies, and fusion proteins.⁴²

Here, we compare PS80's (Figure 1a) effectiveness as an interfacial stabilizer to an alternative surfactant that has been shown to adsorb more strongly to interfaces than both polysorbates and proteins.⁴² This alternative surfactant, *N*-myristoyl phenylalanine-*N*-polyetheramine diamide (FM1000), consists of a saturated hydrophobic tail and a hydrophilic polymeric head group linked together via amide bonds, Figure 1b. Due to the absence of ester bonds in the FM1000 structure, the molecule is less prone to enzymatic degradation as compared to polysorbates. Oxidation pathways are similar to those found in PS80 and poloxamer due to the presence of polyether hydrophiles in all molecules, and oxidation mitigation strategies used for PS80 and poloxamer could similarly be leveraged for FM1000.³² Initial studies on the ability of FM1000 to prevent protein aggregation have been reported by Hanson et al.⁴³ and Katz et al.^{42,44}

To examine this molecular hypothesis, we use pendant bubble tensiometry and X-ray reflectivity (XRR). Prior studies from our group⁴⁵ on PS80 applied similar tools to quantify the concentration of the surfactant required to protect proteins from interfaces as a function of different mAbs' surface activities. For a fixed mAb concentration, a more surface-active mAb required a fivefold greater PS80 concentration as compared to the low surface-active mAb at a given mass (or molar) concentration. We extend our earlier study using a range of both mAb and surfactant (PS80 and FM1000) concentrations to assess the differences in interfacial behavior. Due to the ability of FM1000 to lower the surface tension at a faster rate for a given mass concentration than PS80, we found that a constant concentration of FM1000 was sufficient to prevent the adsorption for a range of protein concentrations.

On the other hand, the PS80 levels required varied with the protein bulk concentration. These results provide a molecular-level mechanistic understanding of different surfactants' abilities to prevent protein adsorption, opening doors for alternative surfactants for therapeutic formulations. Additionally, this study shows that for chemically different surfactants, the critical micelle concentration (CMC) of the surfactant is not the driving force for protein drug product stabilization.

MATERIALS AND METHODS

Materials. The mAb used for this study was provided by Bristol–Myers Squibb. PS80 (average molecular weight of 1310 g/mol) was provided by NOF Corporation and is an all-oleate surfactant with minor amounts of heterogeneous fatty acid ester. FM1000 (average molecular weight of 1400 g/mol) was synthesized as previously reported and stored as a frozen aqueous stock solution.⁴³ It is a relatively monodisperse material synthesized from purified myristic acid. The polydispersity of the FM1000 is driven by the dispersity of the polyether hydrophile and is less than 1.1. mAb belongs to the IgG4 family with a molecular weight of 144,481 Da and is supplied as a stock solution of 10 mg/mL in 20 mM histidine buffer at pH 6. The stock solution is stored at -60°C in small aliquots and thawed as needed.

METHODS

Preparation of Diluted Solutions. The 20 mM histidine pH 6 buffer and the stock mAb and surfactant solutions are filtered using 0.22 μm polyvinylidene fluoride filters prior to usage in making diluted solutions. The mixed mAb + PS80 and mAb + FM1000 solutions are prepared using the formulated stock solutions of the respective surfactants in 20 mM of histidine buffer. All solutions are made with deionized water filtered with an EMD Millipore Milli-Q system (Burlington, MA). The mAb concentration in the diluted solutions is verified using the extinction coefficient of 1.50 mL mg^{-1} cm^{-1} measured at 280 nm.

Dynamic Tension Measurements. The adsorption of proteins or surfactants onto the air/water interface is studied using a pendant bubble tensiometer (Attension Theta, Biolin Scientific, Stockholm, Sweden). An inverted needle (16 gauge) is used to inflate a pendant-shaped air bubble (volume \approx 22 μL) at the tip of the needle in a quartz cuvette filled with mAb or surfactant or mAb + surfactant solution. The needle is connected to a 500 μL gas-tight Hamilton syringe placed on a syringe pump (PHD, Harvard Apparatus). The pump is programmed to push air through the syringe. As molecules adsorb to the surface, the change in bubble shape due to adsorption is recorded (6.5 frames per second for the first 5×10^3 s and then at 3.5 frames per second for another 5×10^3 s). The recorded bubble images are then fitted to the Young–Laplace equation to calculate dynamic surface tension as a function of time. The needle, syringe, and the quartz cuvette are cleaned with DI water and sonicated for 60 min, followed by verifying the surface tension of a clean air/water interface [(72.5 ± 0.3) mN/m] before each experiment. All measurements are performed at room temperature (20 ± 3) $^{\circ}\text{C}$.

XRR Measurements. The XRR studies reported in this study were performed at NSF's ChemMatCARS, station 15 ID-C experimental hut at the Advanced Photon Source in Argonne National Laboratory (Argonne, IL).^{46–48} The wavelength of the X-rays used is 1.24 Å , and all X-ray data

are collected using a PILATUS3 200 K area detector. A custom-built Langmuir trough insert ($7 \times 3 \times 0.1$ cm) is used to fit the existing X-ray setup at the beamline. The buffer solution used to dilute mAb or surfactant solutions is degassed for at least 1 h before the setup. Solutions are freshly prepared and gently poured onto the Langmuir trough, and the formation of this liquid layer is taken to be $t = 0$ for the adsorption process during XRR measurements. The trough is in a chamber in the X-ray hut room, and the chamber requires evacuation before the experiment can be initiated. This process requires 50 min. A scan of the surface then takes 50 min. Hence, after completion of the scan, approximately 100 min or 6.0×10^3 s had elapsed from the moment the air/liquid interface of the trough was formed. The X-ray signal obtained reflects the adsorption process at a stage of approximately 6.0×10^3 s from the formation of the clean interface. All the measurements are carried out at room temperature (22 ± 1) $^{\circ}\text{C}$. The details of the XRR data analysis are provided in the [Supporting Information](#).

Agitation Studies. 1 mg/mL stock solutions of FM1000 and PS80 in 20 mM histidine at pH 6 are used to prepare a series of protein solutions containing 2.5 mg/mL of mAb and the following concentrations of surfactant: 0.1, 0.05, 0.01, 0.005, 0.001, and 0.0005 mg/mL. 5 mL of DWK Life Sciences CompletePAK serum vials are filled with 3 mL/vial solution and capped with a 20 mm stopper. Capped vials are oriented on their sides and subjected to reciprocal shaking (180 strokes/min) for 24 h at room temperature. After shaking, 1.4 mL/vial is transferred to individual wells of a water-washed 96-well deep-well plate and analyzed by micro-flow imaging (MFI) (ProteinSimple). Image-based sub-visible particle differentiation is performed within the software, and resultant data are analyzed in JMP Pro 15.0.0. All samples are run in triplicate.

Contact Angle Measurements. C6-150 silicone slabs (1×3.5 cm), courtesy of DuPont, are placed into open Petri dishes within Nalgene containers and surrounded by water to ensure minimal evaporation of the sample. The silicone used for this work is chemically similar (and therefore would have the same surface energetics) to that which is used to coat syringes, only cross-linked to form a solid slab. It is also the same material that is used to form pharma-relevant silicone tubing. No water entered the Petri dishes or made physical contact with the slabs. 1.5 mL of protein solution containing 2.5 mg/mL of mAb with or without FM1000 or PS80 (at 0.05, 0.02, 0.01, 0.005, 0.001, 0.0005, 0.0003, 0.0002, 0.0001, 0.00005, or 0.00001 mg/mL) is prepared in 20 mM L histidine at pH 6 and added to the surface of the silicone slabs. The containers are then sealed and set aside at room temperature for 24 h. Formulations are then removed from the slabs using the capillary action of a paper towel, followed by drying with nitrogen. 3 μL droplets of Milli-Q water ($n = 5$) were manually dispensed via a pipette onto the surface of the slab, and images of droplets at equilibrium were recorded for analysis. Fouling is measured by a decrease in contact angle, and the results are analyzed in JMP Pro 15.0.0.

RESULTS AND DISCUSSION

Dynamic Surface Tension Measurements. Pendant bubble tensiometry is used to examine the dynamic decrease in surface tension as the mAb or surfactant adsorbs from bulk solution onto the clean air/water interface. The mAb surface tension relaxation is discussed first, followed by surfactant

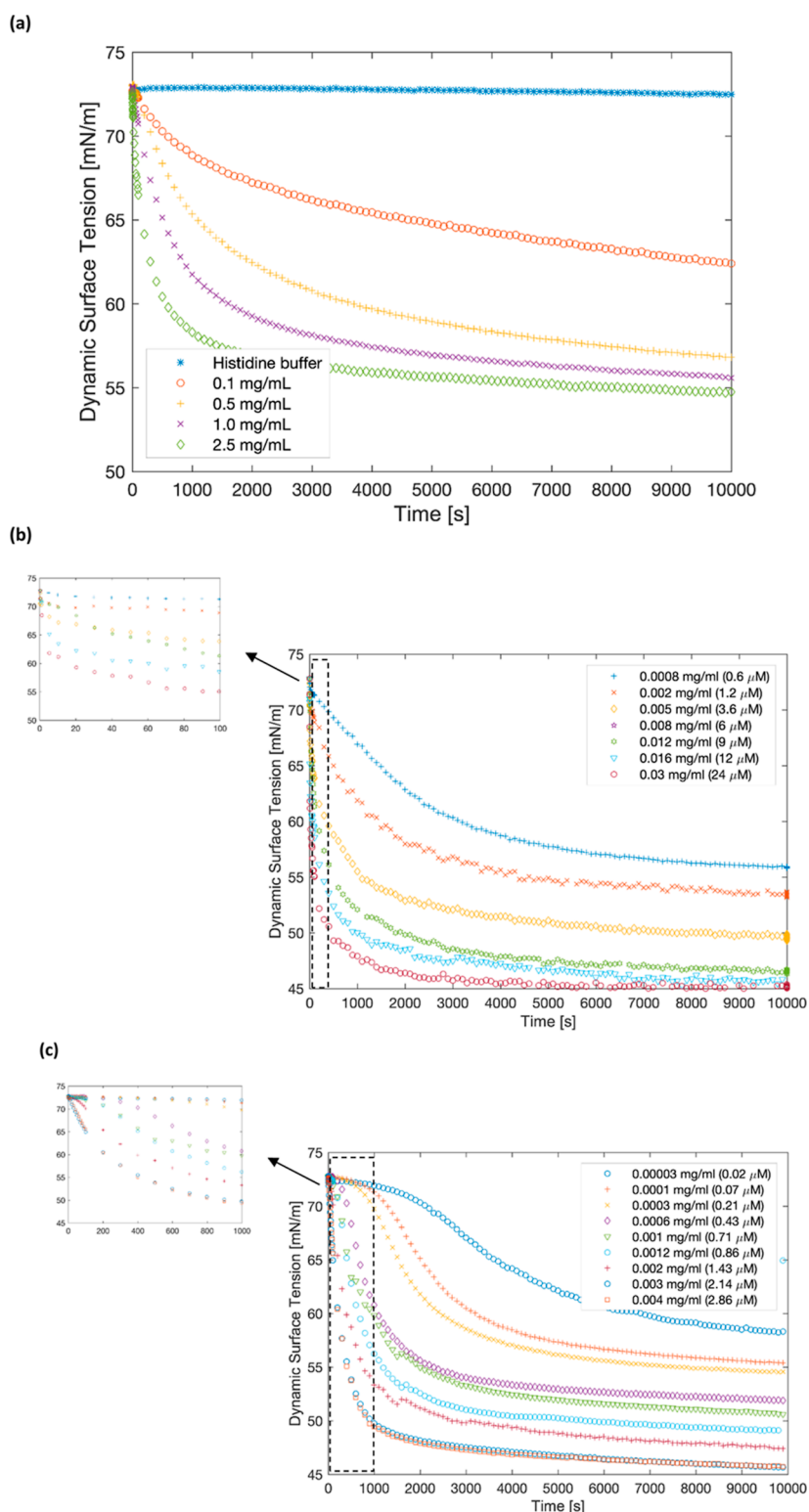


Figure 2. Dynamic surface tension measurement profiles for (a) mAb, (b) PS80, and (c) FM1000 using a pendant bubble tensiometer. As mAb and surfactant molecules adsorb to the pendant bubble interface, a reduction in the surface tension is recorded for 1.0×10^4 s. For mAb, the tension measurement is recorded for 1.0×10^{-1} to 2.5 mg/mL; for PS80, tension is recorded for the concentration range of 8.0×10^{-3} to 3.0×10^{-2} mg/mL (0.6 – $24 \mu\text{M}$), whereas for FM1000, surface tension is reported for a bulk concentration of 3.0×10^{-5} to 4.0×10^{-3} mg/mL (0.02 – $2.86 \mu\text{M}$). All solutions are prepared from the mAb and surfactant stock solution in 20 mM histidine buffer at pH 6.

tension profiles. Figure 2a shows the dynamic tension profile of mAb alone as it adsorbs from the bulk solution to the air/water interface along with the histidine buffer tension profile. The buffer solution used for preparation of diluted mAb or

surfactant or mAb + surfactant systems is not surface active and has an equilibrium surface tension value of 72.5 mN/m (similar to the clean air/water interface surface tension). Diluted mAb solutions in histidine buffer ranging from $1.0 \times$

10^{-1} to 2.5 mg/mL are studied over the time period of 1.0 – 1.0×10^4 s. The mAb concentration used in this study is similar to typical intravenous (IV) administration dosages where concentrated protein solutions (100–150 mg/mL) are approximately diluted 1000-fold.^{49,50} The surface tension profile is similar to that reported for globular proteins⁵¹ and other mAbs.⁴⁵ As the bulk concentration increases, the surface tension decreases in a way similar to that observed for low molecular-weight surfactants, PS80 (Figure 2b) and FM1000 (Figure 2c). For all the mAb concentrations studied, the surface tension decreases and reaches a quasi-equilibrium value as molecules adsorb to the surface. At long times, the tension continues to decrease and does not achieve an equilibrium value, indicating irreversible adsorption of mAbs upon adsorption due to unfolding or slow rearrangements of the adsorbed mAbs.^{45,52}

The dynamic surface tension measurements are executed at bulk concentrations of surfactants from 8.0×10^{-4} to 3.0×10^{-2} mg/mL (or 0.6–24 μ M for PS80, Figure 2b) and 3.0×10^{-5} to 4.0×10^{-3} mg/mL (or 0.02–2.86 μ M for FM1000, Figure 2c) over the time period of 1.0 – 1.0×10^4 s. All solutions are prepared from the respective surfactant stock solution in 20 mM histidine buffer at pH 6. The dynamic surface tension profile of surfactants alone is used to determine the relative rate of the surfactant molecules adsorbing to the air/water interface to inhibit subsequent protein adsorption. Figure 2b,c shows that at the same bulk concentration of PS80 or FM1000, FM1000 lowers the surface tension much faster as compared to PS80. For instance, at a bulk concentration of 2.0×10^{-3} mg/mL, the tension relaxation for FM1000 reaches an equilibrium value of 47 mN/m as opposed to 52 mN/m for PS80 in 1.0×10^4 s. This indicates that FM1000 is more surface active than PS80 for the same mass concentration, and the interface is populated more rapidly by FM1000 molecules, consistent with previous results.⁴² Additionally, Figure 2c shows that for lower concentrations of FM1000 (3.0×10^{-5} to 6.0×10^{-4} mg/mL), an early induction period in the surface tension is observed where the tension remains equal to the tension of the clean air/water interface before an actual decrease in the surface tension. As FM1000 bulk concentration increases, the induction period shortens and eventually disappears (see the insert for Figure 2c) with an immediate reduction in the tension.

Typically, the CMC of surfactants plays a key role in the rate of surface adsorption. Equilibrium surface tension values, which are based on long-time dynamic tension, are also a function of bulk surfactant concentration (Figure S1). These results show that as the bulk concentration increases, the equilibrium surface tension value decreases for both the surfactants. For FM1000, the plot indicates a CMC value of 3.0×10^{-3} mg/mL (2.14 μ M). The CMC value of FM1000 is slightly different than that reported by Hanson et al. (denoted as 14FM1000), where dynamic light scattering was used to measure the CMC of FM1000 in 0.9% saline. We believe this difference is due to the different solution matrices and techniques used in this study.⁴³

Our earlier study reported a CMC of 1.6×10^{-2} mg/mL (12 μ M) for PS80,⁴⁵ and PS80's CMC value is approximately five times higher than the CMC value for FM1000, indicating that a lower concentration of FM1000 would be sufficient to form a surfactant monolayer onto the surface. Additionally, a Langmuir adsorption fit to the constructed equilibrium surface tension as a function of bulk concentration indicated a

maximum packing of surfactant concentration (Γ_{∞}) of around 1.88 mg/m² for PS80 and 1.45 mg/m² for FM1000. Equivalently, the area per molecule of the surfactant ($A_s = 1/\Gamma_{\infty}$) is calculated to be 115 Å²/molecule and 187 Å²/molecule for PS80 and FM1000, respectively. A higher value of A_s for FM1000 further indicates a larger “footprint” of the FM1000 molecule at the interface compared to PS80. In other words, fewer FM1000 surfactant molecules (or less bulk FM1000 concentration) would be needed to populate the air/water surface and inhibit protein adsorption.

Using dynamic surface tension measurements, one can predict the relative rates of adsorption of different surfactants. As discussed in the introduction, surfactants are added in protein formulations to stabilize the surface, inhibiting protein adsorption. However, even though surfactants are more surface active than proteins, at a high enough protein concentration, hydrophobic proteins can compete with surfactants for the interfacial area.^{11,45} Based on the dynamic surface tension data, a complete mechanistic understanding of protein–surfactant interaction at the air/water interface is not feasible. Additionally, the equilibrium tension data for the mixed protein–surfactant solutions cannot probe whether an adsorbed protein layer is present below the surfactant monolayer. Therefore, a more sensitive technique that can probe the interfacial layer up to 20–40 nm is required. In order to gain a quantitative understanding of interfacial adsorption of the mixed protein–surfactant system, we use XRR measurements.

XRR Measurements. XRR allows one to examine the ensemble average packing of surfactant molecules and the competitive adsorption between surfactants and proteins. Our experiments investigate a series of surfactant concentrations for PS80 and FM1000 to understand the difference in the surface packing of these molecules. Additionally, we fix the protein concentration and vary the surfactant concentration (either PS80 or FM1000) to predict the minimum surfactant concentration required to inhibit protein adsorption onto the air/water interface. Before studying the mixtures of PS80 or FM1000 with the protein, we examined the single component system (surfactant alone and protein alone). As molecules adsorb to the surface, the variation in the electron density, $\rho(z)$, perpendicular to the interface (z) can be determined using XRR. The electron density profile (EDP) can then be integrated in the z direction to calculate the thickness and surface concentration of the adsorbed layer using the known structure of protein, PS80, and FM1000.

The experimental procedure for XRR measurements has been reported in our earlier study.¹¹ Briefly, pure surfactant, pure protein, or the mixed protein–surfactant solution is gently poured onto a custom-built rectangular trough. An adsorbed thin liquid film forms onto the air/water interface due to the dynamic adsorption of molecules from the bulk solution. X-rays from the synchrotron beam are incident at an angle, α onto the planar air/water interface. The reflectivity R is measured as a function of the incident angle, α . The experimental data are reported as the normalized reflectivity, $R(Q_z)/R_F(Q_z)$ as a function of the wave vector transfer, $(Q_z) = (4\pi/\lambda) \sin(\alpha)$ where $R_F(Q_z)$ is the Fresnel reflectivity from an ideally flat air/water interface whose electron density varies as a step-function at the interface, and $\lambda (= 1.24 \text{ \AA})$ is the wavelength of the incident X-ray. The incident angle α is varied to cover the range $0.016 \text{ \AA}^{-1} < Q_z < 0.6 \text{ \AA}^{-1}$. The normalized reflectivity is then fitted using the Parratt method to generate the corresponding EDP ($\rho(z)$) as a function of

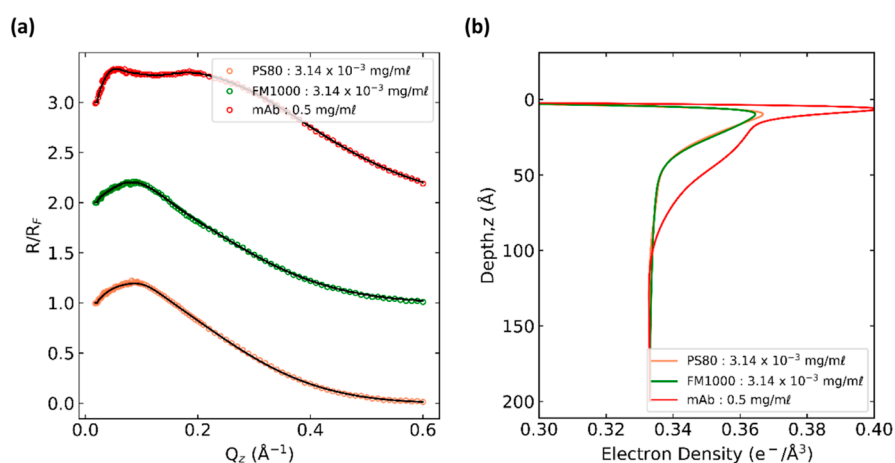


Figure 3. XRR measurements of the adsorbed layers of pure mAb or pure surfactants from bulk solution onto the air/water interface. (a) Representative normalized XRR profiles, R/R_F , as a function of wave vector transfer, Q_z , (symbols) and Parratt fits to the reflectivity profile (solid line) for PS80 (orange), FM1000 (green), and mAb (red). XRR data for surfactants (PS80 or FM1000) show a single peak, whereas the mAb profile shows multiple peaks for $Q_z < 0.2$ \AA . The upper two XRR curves are shifted for clarity; $R/R_F \rightarrow 1$ as $Q_z \rightarrow 0$ for all measurements. (b) Corresponding EDPs as a function of interfacial depth, z , obtained from the reflectivity fits for PS80 (orange), FM1000 (green), and mAb (red), as derived from (a).

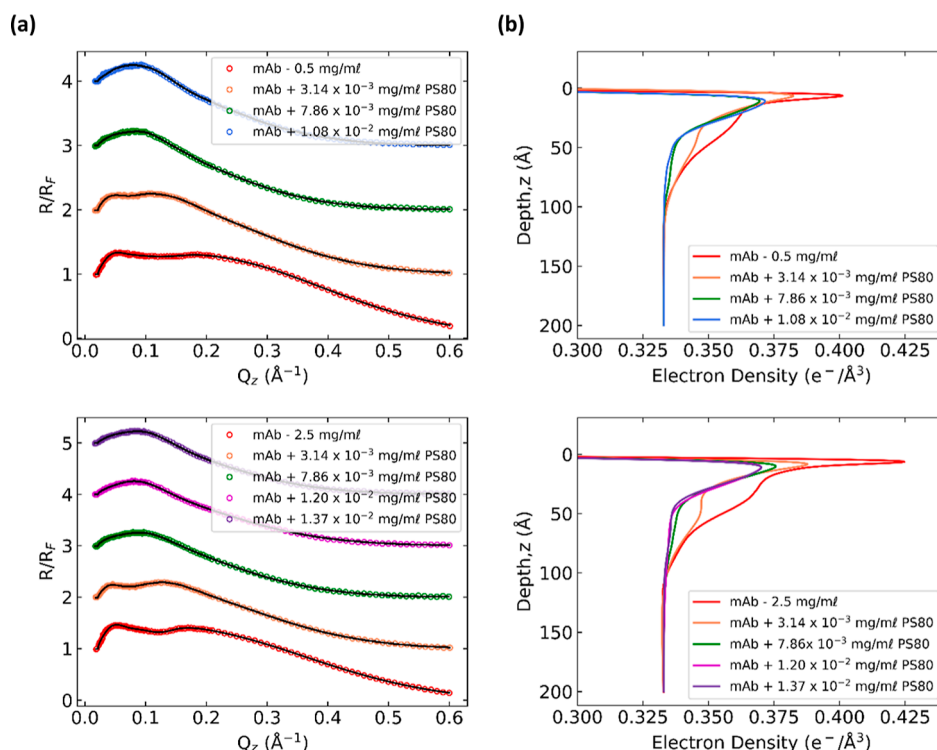


Figure 4. XRR measurements of the adsorbed layers from competitive adsorption of mAb (0.5 and 2.5 mg/mL) and PS80 from bulk solution onto the air/water interface. (a) Normalized XRR profiles, R/R_F , as a function of wave vector transfer, Q_z , (symbols) and Parratt fits to the reflectivity profile (solid line) for mAb (0.5 mg/mL) and PS80 at increasing concentrations (3.14×10^{-3} , 7.86×10^{-3} , and 1.08×10^{-2} mg/mL) in the top panel and mAb (2.5 mg/mL) and PS80 at increasing concentrations (3.14×10^{-3} , 7.86×10^{-3} , 1.20×10^{-2} , and 1.37×10^{-2} mg/mL) in the bottom panel. The XRR curves are shifted for clarity; $R/R_F \rightarrow 1$ as $Q_z \rightarrow 0$ for all measurements. (b) Corresponding EDPs as a function of interfacial depth, z , obtained from the reflectivity fits for the mixed component system derived from (a).

interfacial depth, z . For more details regarding the fitting procedure, see the [Supporting Information](#) text.

The normalized reflectivity $R(Q_z)/R_F(Q_z)$ as a function of Q_z for pure surfactants (PS80 or FM1000) is reported in [Figure 3a](#). The corresponding EDP curves are shown in [Figure 3b](#). XRR measurements for pure surfactants are performed for bulk concentrations in the range of 3.14×10^{-3} to 1.37×10^{-2} mg/mL (additional surfactant concentration XRR profiles are

reported in the [Supporting Information](#), Figures S2 for PS80 and S3 for FM1000). A broad maximum in the reflectivity measurement of pure surfactant is observed for the studied concentration range. This can be attributed to a similar molecular architecture for both PS80 and FM1000. For the case of a protein-alone system, a representative reflectivity profile at a bulk concentration of 0.5 mg/mL is shown in [Figure 3a](#). The corresponding EDP is reported in [Figure 3b](#). As

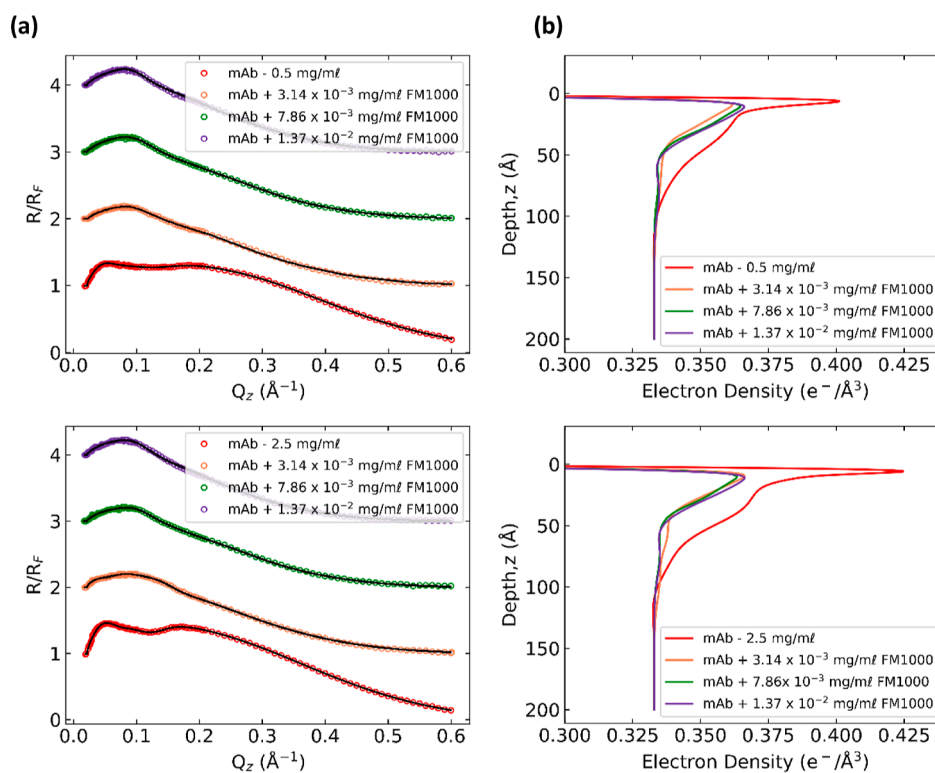


Figure 5. XRR measurements of the adsorbed layers from competitive adsorption of mAb (0.5 and 2.5 mg/mL) and FM1000 from bulk solution onto the air/water interface. (a) Normalized XRR profiles, R/R_F , as a function of wave vector transfer, Q_z , (symbols) and Parratt fits to the reflectivity profile (solid line) for mAb (0.5 mg/mL) (upper panel) and mAb (2.5 mg/mL) (bottom panel) with increasing concentrations of FM1000 (3.14×10^{-3} , 7.86×10^{-3} , and 1.37×10^{-2} mg/mL). The XRR curves are shifted for clarity; $R/R_F \rightarrow 1$ as $Q_z \rightarrow 0$ for all measurements. (b) Corresponding EDPs as a function of interfacial depth, z , obtained from the reflectivity fits for the mixed component system derived from (a).

opposed to only a broad maximum for the case of surfactants, the adsorbed protein profile shows two maxima peaks at lower Q_z . These conclusions were also reached in a study reported by our group for a different class of protein and PS80.⁴⁵

Figures 4 and 5 report the normalized reflectivity, Parratt fits, and EDP for the competitive adsorption between mAb + PS80 (Figure 4) and mAb + FM1000 (Figure 5). The mAb concentration was studied at 0.5, 1.0, and 2.5 mg/mL. The surfactant bulk concentration for PS80 ranges from 3.14×10^{-3} to 1.94×10^{-3} mg/mL, whereas for FM1000, the surface concentration ranges from 3.14×10^{-3} to 1.37×10^{-2} mg/mL. For discussion, protein concentrations of 0.5 and 2.5 mg/mL are used (see Supporting Information for results corresponding to protein concentrations at 1.0 mg/mL, Figures S4 and S5). Figure 4a (top row) shows that for a protein concentration of 0.5 mg/mL, as PS80 concentration increases, the two maxima peaks observed for proteins converge to a single broad maximum peak, indicating PS80 dominating the surface (see overlapped XR curves, Figure S6 of Supporting Information). For a PS80 concentration of 3.14×10^{-3} mg/mL, a shift in the second maxima of the reflectivity profile to lower Q_z is observed. This is attributed to the adsorption of PS80 molecules that have competitively adsorbed along with the protein molecules, resulting in the formation of mixed layers that cause a shift to lower Q_z . PS80 surfactant molecules will reach the clean surface rapidly due to faster diffusion of PS80 molecules than proteins from the bulk solution to the air/water interface. However, at a low enough concentration of PS80 (3.14×10^{-3} mg/mL), the bulk supply of surfactants is not sufficient to completely prevent the adsorption of proteins to

the surface (cf. the comparison graph S6a in the Supporting Information). A similar conclusion can be reached by comparing the EDP of the two-component system (Figure 4b, top row). As the PS80 concentration is increased to 7.86×10^{-3} mg/mL, the reflectivity (or EDP) shows a broad maximum similar to that of pure PS80's alone reflectivity profile at the same bulk concentration (cf. comparison graph S6b in the Supporting Information). This indicates that the PS80 molecules have blocked the surface, inhibiting any further protein adsorption. Similarly, for a protein concentration of 1.0 mg/mL, the surfactant concentration of 7.86×10^{-3} mg/mL is sufficient to prevent protein adsorption (Figure S4a,b and Table S3). As protein concentration is increased to 2.5 mg/mL, a surfactant concentration greater than 1.20×10^{-2} mg/mL is required to inhibit protein adsorption (Figure 4a,b, bottom row). As protein concentration increases, the number of protein molecules competing for the surface also increases. Therefore, to overcome the flux of proteins reaching the surface, a sufficiently higher surfactant concentration is required to surpass the protein flux and form a layer onto the surface, thereby preventing protein adsorption.

Similar experiments are performed with the same protein concentrations but using FM1000 as the surfactant. The FM1000 concentration of 3.14×10^{-3} mg/mL showed protein-like XRR features at lower Q_z , indicating the presence of a mixed layer on the surface regardless of the protein concentration (see overlapped XR curves, Figure S7a of Supporting Information). However, at this surfactant concentration, compared to the protein + PS80 system, from the qualitative representation of the measured reflectivity profiles

(the presence of two distinct maxima peaks), the interface for the protein + FM1000 system has less protein present (cf. comparison graph S7a and the subset plot in the [Supporting Information](#)). Interestingly, for all the studied protein concentrations of 0.5–2.5 mg/mL, the FM1000 concentration equal to or greater than 7.86×10^{-3} mg/mL is sufficient to prevent protein adsorption:

The PS80 concentration necessary to prevent protein adsorption is below its CMC value, while all of the FM1000 concentrations studied are above its CMC value ([Table 1](#)). For

Table 1. Surfactant Concentration in Terms of CMC Values of PS80 and FM1000

surfactant conc. mg/mL	PS80 \times CMC	FM1000 \times CMC
3.14×10^{-3}	0.20	1.05
7.86×10^{-3}	0.50	2.62
1.37×10^{-2}	0.86	4.57

FM1000 surfactant concentrations greater than 7.86×10^{-3} mg/mL, sufficient micellar aggregates are present in the bulk solution. However, for a FM1000 bulk concentration of 3.14×10^{-3} mg/mL ($1.05 \times$ CMC) that corresponds to the onset of CMC, it will have fewer micellar aggregates as compared to monomers. This indicates that even if the surfactant concentration is above its CMC value, protein adsorption can still be dominant. We believe, as suggested by these data, that the inhibition of protein adsorption onto surfaces has to do with the absolute concentration of surfactant required in the solution (micellar or free monomers) rather than a function of the percentage of CMC.

Adsorbed Layers of PS80 and FM1000. The surface concentration of adsorbed PS80 (Γ_{PS80}) or FM1000 layers (Γ_{FM1000}) onto the air/water interface is calculated using the EDPs ([Figures 3b](#), [S2b](#), and [S3b](#); for details see [Supporting Information](#) text). The corresponding equivalent area per molecule of the PS80 ($A_{\text{PS80}} = 1/\Gamma_{\text{PS80}}$) or FM1000 ($A_{\text{FM1000}} = 1/\Gamma_{\text{FM1000}}$) surfactant is also reported in [Table 2](#). Error bars are

Table 2. Surface-Adsorbed Amounts and Area per Molecule for Pure Layers of PS80 and FM1000

surfactant conc. mg/mL	PS80		FM1000	
	Γ_s mg/m ²	A_s Å ²	Γ_s mg/m ²	A_s Å ²
3.14×10^{-3}	1.48 ± 0.08	147 ± 7	0.61 ± 0.09	378 ± 61
7.86×10^{-3}	2.09 ± 0.09	104 ± 5	0.79 ± 0.02	295 ± 6
1.37×10^{-2}	2.28 ± 0.12	96 ± 5	0.95 ± 0.06	244 ± 15

calculated based on one standard deviation from the best-fit value. For both PS80 and FM1000, as surfactant concentration increases, the surface concentration increases due to an increase in the number of surfactant molecules adsorbed to the air/water interface. Γ_{PS80} increases with an increase in PS80 bulk concentration up to the CMC value of PS80, where it becomes constant. The surface concentration of PS80 is in the range of 1.48–2.28 mg/m² for the concentration range of 3.14×10^{-3} to 1.37×10^{-2} mg/mL ([Tables 2](#) and [S2](#) of [Supporting Information](#)). For the FM1000 surfactant, the surface concentration Γ_{FM1000} is between 0.61 and 0.95 mg/m² ([Table 2](#)) for the concentration range of 3.14×10^{-3} to 1.37×10^{-2} mg/mL. The maximum surface packing value for PS80 ($\Gamma_{\infty, \text{PS80}}$) or FM1000 ($\Gamma_{\infty, \text{FM1000}}$) from XRR measurement

(2.28 mg/m² for PS80 and 0.95 mg/m² for FM1000) is in approximate agreement with that obtained from dynamic tension measurements (1.88 mg/m² for PS80 and 1.25 mg/m² for FM1000) (see [Figure S1](#) and [Supporting Information](#) text). The recorded surface concentration of FM1000 is two times lower than that of PS80. In other words, the area per molecule for FM1000 is approximately two times greater than PS80 for the bulk concentration of 1.37×10^{-2} mg/mL, with fewer FM1000 molecules adsorbing to the surface. These data indicate that FM1000 molecules are able to block a larger percentage of the interfacial area upon adsorption to the surface. These data also support an earlier hypothesis by Hanson et al., where along with the hydrophobic tail, adsorption and rearrangement of PEO, PPO or phenylalanine regions is also possible, causing a further decrease in the surface tension value while expanding the surface coverage of each individual surfactant molecule.⁴³

Adsorbed Layers of Protein. The surface concentration of the adsorbed protein layer (Γ_p) is calculated based on its EDP ([Figures 3b](#), [4b](#), and [5b](#); for details see [Supporting Information](#) text). The values are reported in [Table 3](#) and are

Table 3. Surface-Adsorbed Amounts and Area per Molecule for Pure Layers of mAb

protein conc. mg/mL	Γ_p mg/m ²	A_p Å ²
0.5	1.15 ± 0.06	$20,781 \pm 994$
1.0	1.54 ± 0.04	$15,593 \pm 411$
2.5	1.81 ± 0.06	$13,280 \pm 410$

in the range of 1.15–1.81 mg/m² for the bulk concentration of 0.5–2.5 mg/mL protein. The area per molecule for this protein is in the range of 13,280–20,781 Å². Based on the homology model ([Figure S8](#)), the dimensions of the mAb protein molecules are $150 \times 125 \times 55$ Å with the Fab thickness of 40 Å and an Fc domain of 55 Å. Molecular orientations in flat-on, side-on, or end-on have been reported for protein molecules on hydrophobic surfaces.⁵² For a perfectly flat-on orientation, the area per molecule would correspond to (150×125) 18,750 Å², whereas side-on (125×55) or end-on (150×55) orientations would be 6875 Å² and 8250 Å², respectively. Based on the XRR-calculated area per molecule values ([Table 3](#)), the protein is adsorbed in a spaced-out flat-on orientation at 0.5 mg/mL. As protein concentration increases to 2.5 mg/mL, the area per molecule decreases to $13,280 \pm 410$ Å². This value is lower than the area per molecule for the maximum packing of the flat-on orientation (18,750 Å²) but higher than that for the side-on (6875 Å²) or end-on (8250 Å²) orientation. Prior studies using homology modeling by our group have indicated that the adsorbed layer surface population could consist of a mixture of all three orientations (flat-on, side-on, and end-on).⁵²

Mixed Adsorbed Layers. The qualitative comparison of XRR profiles of protein concentration of 0.5 and 2.5 mg/mL with PS80 or FM1000 is discussed in detail (see [Figures S4](#) and [S5](#) for protein concentration results at 1.0 mg/mL with PS80 and FM1000, respectively, in the [Supporting Information](#)). The reflectivity and the corresponding EDPs for the mixed mAb + surfactant system exhibit characteristics from the individual surfactant and mAb systems. The co-adsorbed interfacial layer at the air/water interface can be modeled as a combination of pure surfactant and pure protein component with a proper weighting factor a , where a is the relative percent

Table 4. Surface-Adsorbed Amounts, Area per Molecule, and Relative Percent Surface Coverage of mAb in Mixed Layers of mAb and PS80

mAb conc. mg/mL	PS80 conc. mg/mL	Γ_p mg/m ²	A_p Å ²	Γ_s mg/m ²	A_s Å ²	% <i>a</i> obtained from fitting for protein coverage
0.5	3.14×10^{-3}	0.53 ± 0.15	$44,995 \pm 9667$	0.81 ± 0.16	270 ± 66	46
	7.86×10^{-3}	0		2.05 ± 0.10	106 ± 6	
	1.08×10^{-2}	0		2.45 ± 0.12	89 ± 2	
2.5	3.14×10^{-3}	0.54 ± 0.03	$44,735 \pm 2378$	1.06 ± 0.06	205 ± 11	29
	7.86×10^{-3}	0.21 ± 0.01	$113,487 \pm 1446$	1.85 ± 0.09	117 ± 6	
	1.20×10^{-2}	0.07 ± 0.02	$339,405 \pm 86,183$	1.93 ± 0.12	113 ± 2	
	1.37×10^{-2}	0		2.28 ± 0.17	103 ± 8	

Table 5. Surface-Adsorbed Amounts, Area per Molecule, and Relative Percent Surface Coverage of mAb in Mixed Layers of mAb and FM1000

mAb conc. mg/mL	FM1000 conc. mg/mL	Γ_p mg/m ²	A_p Å ²	Γ_s mg/m ²	A_s Å ²	% <i>a</i> obtained from fitting for protein coverage
0.5	3.14×10^{-3}	0.12 ± 0.01	$202,662 \pm 14,911$	0.48 ± 0.15	489 ± 119	10
	7.86×10^{-3}	0		0.71 ± 0.08	245 ± 21	
	1.37×10^{-2}	0		1.09 ± 0.18	212 ± 30	
2.5	3.14×10^{-3}	0.29 ± 0.12	$82,722 \pm 62,366$	0.52 ± 0.12	450 ± 87	15
	7.86×10^{-3}	0		0.76 ± 0.02	307 ± 6	
	1.37×10^{-2}	0		0.95 ± 0.07	244 ± 17	

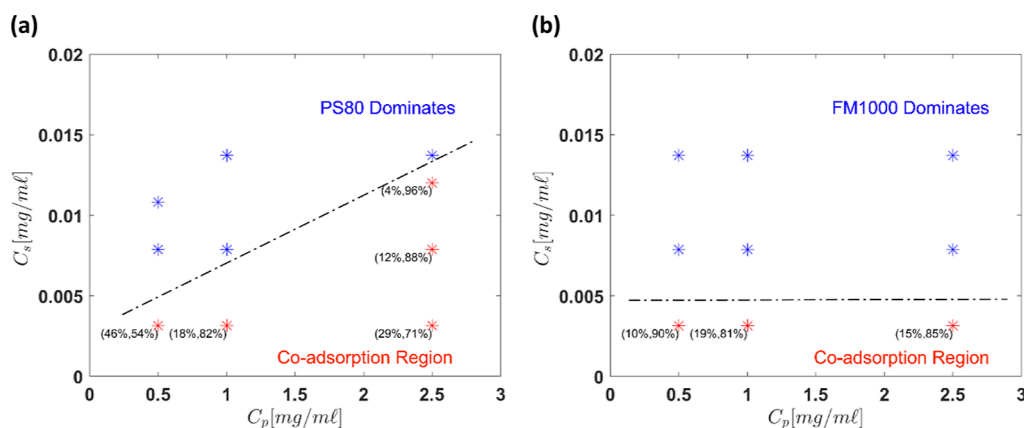


Figure 6. Minimum surfactant concentration for a given bulk mAb concentration to inhibit mAb adsorption onto the surface, derived from XRR measurements. The percent coverage for the co-adsorbed layers (red symbols) as determined from reflectivity fits where the first number indicates protein coverage, *a*, followed by surfactant coverage, (1 - *a*). Blue symbols are points where no measurable protein is adsorbed to the surface. (a) As the mAb concentration increases from 0.5 to 2.5 mg/mL, the PS80 concentration to prevent the adsorption of mAbs onto the air/water interface also increases. (b) Fixed value of FM1000 concentration is required to inhibit mAb adsorption. The black dashed line is shown to provide a guide for the reader.

surface coverage of mAb, and 1 - *a* represents the surfactant coverage. Using *a* as the only fitting parameter for fitting the co-adsorbed reflectivity profiles gives reasonable fits for the mAb + surfactant data sets.⁴⁵ The mAb and surfactant percent surface coverage [*a* %, (1 - *a*)%] are reported in Tables 4, 5, S3, S4 and Figure 6. The calculations for the surface-adsorbed amount for the mixed system are detailed in the Supporting Information text. We consider first the mixed layers of protein + PS80 with a fixed protein concentration of 0.5 mg/mL. At the lowest PS80 concentration of 3.14×10^{-3} mg/mL, the surface concentration of protein in the mixed layer decreased to 0.53 ± 0.15 and 0.81 ± 0.16 mg/m² for the surfactant (corresponding to a coverage ratio of mAb/PS80 = 46:54%, Figure 6). The pure protein surface concentration at 0.5 mg/mL is 1.15 ± 0.06 mg/m² (Table 3). Therefore, in the presence of PS80, a lower value in the protein surface concentration in the mixed layer as compared to the pure protein system is indicative of PS80 blocking some of the

interfacial area. The PS80 surface concentration at this bulk concentration corresponds to 1.48 ± 0.08 mg/m², and the surface concentration of PS80 in the two-component system is not as high as in the pure PS80 system, indicating co-adsorbed layers of both mAb and PS80 on the surface. This is due to fewer surfactant molecules in the solution being available to prevent mAb adsorption. As the surfactant concentration increases to 7.86×10^{-3} mg/mL, no measurable protein is detected on the surface. The surfactant concentration is equal to its saturation value of 2.05 ± 0.10 mg/m², indicating a complete blockage of protein molecules to the surface. A further increase in the PS80 concentration gives the corresponding saturation value of pure PS80. This indicates that a concentration greater than 7.86×10^{-3} mg/mL is sufficient to prevent protein adsorption with a bulk concentration of 0.5 mg/mL.

As protein concentration increases, the number of protein molecules adsorbing to the surface also increases, resulting in

an increase in protein surface concentration (Table 3). At a protein concentration of 2.5 mg/mL, a PS80 concentration of 7.86×10^{-3} mg/mL is not sufficient to prevent protein adsorption. The protein surface concentration decreases further to 0.21 ± 0.01 mg/m², and the PS80 surface concentration increases to 1.85 ± 0.09 mg/m². In terms of the surface coverage, the mAb/PS80 ratio is 12:88%, indicating residual protein on the surface. The surfactant concentration has not reached its saturation value of 2.09 mg/m² for this bulk concentration. A further increase in the surfactant concentration to 1.20×10^{-2} mg/mL inhibits the protein adsorption by a factor of 3 from the value of the pure protein layer. The surfactant concentration further increases to 1.93 ± 0.12 mg/m², but a small amount of residual protein still exists (4% mAb). With a further increase in the PS80 concentration to 1.37×10^{-2} mg/mL, no measurable amount of mAb is detected, and the surfactant coverage of PS80 is 100%; the surface-adsorbed amount of PS80 is precisely its saturation value of 2.28 ± 0.17 mg/m². This indicates complete blocking of mAb molecules to the air/water interface. Therefore, with an increase in mAb bulk concentration, PS80 concentration also must increase to prevent mAb adsorption.

For mixed layers of FM1000 at 3.14×10^{-3} mg/mL and mAb protein at 0.5 mg/mL, protein adsorption is inhibited by 10-fold from the value of the pure protein layer (1.15 ± 0.06 mg/m²) as compared to only twofold in the presence of PS80 (0.53 ± 0.15 mg/m²). The FM1000 surface concentration was recorded to be 0.48 ± 0.15 mg/m². The tendency of FM1000 molecules to inhibit protein adsorption at this low bulk concentration can be attributed to its higher area per molecule than PS80, suggesting that fewer FM1000 molecules are required to block the surface, preventing protein adsorption, although some residual protein is still present on the surface (0.12 ± 0.01 mg/m²). With an increase in FM1000 concentration to 7.86×10^{-3} mg/mL, no measurable protein is detected. The surfactant surface concentration is equal to its saturation value of 0.71 ± 0.08 mg/m². Similarly, an FM1000 concentration of 1.37×10^{-2} mg/mL completely blocks protein adsorption onto the surface. As protein bulk concentration increases to 2.5 mg/mL with FM1000 concentration at 3.14×10^{-3} mg/mL, protein adsorption is inhibited by fourfold compared to the adsorption in the pure protein system. Even though the protein bulk concentration is increased by five times, the FM1000 concentration of 7.86×10^{-3} mg/mL is still sufficient to prevent protein adsorption. In comparison, a PS80 concentration of four times higher bulk concentration ($>1.20 \times 10^{-2}$ mg/mL) is necessary to prevent the protein adsorption at the same bulk concentration. As noted earlier, FM1000 concentrations used for this study are above FM1000's CMC. In contrast, all concentrations of PS80 used for the study are below PS80's CMC (Table 1). This shows that CMC is not a critical factor to indicate its ability to inhibit protein adsorption. CMC is a fine comparative measurement to use when working with chemically similar structures. However, for the case of PS80 and FM1000, CMC is not the tool to use due to the difference in their structures.

A summary of the minimum surfactant concentration (C_s) necessary to be present in a mAb formulation for a given protein bulk concentration (C_p) is shown in Figure 6. The qualitative comparison of XRR profiles and the calculation of surface-adsorbed amounts and area per molecule for pure and mixed component systems provide insights into the mechanism for preventing mAb adsorption for two different

surfactants. Our results show that at similar surfactant concentrations, compared to PS80, lower FM1000 concentrations can be used to inhibit protein adsorption at 2.5 mg/mL protein. There are two possible reasons for this difference. First, even though the FM1000 surfactant concentration is above the CMC value, which would indicate a lower number of free monomers in solution, a sufficient number of monomers are still present in the bulk solution to adsorb to the surface, blocking proteins from adsorbing. Perhaps rather than free monomers depositing on the interface, micelles traffic to the interface where many monomers are delivered at once. While the PS80 concentration necessary to block mAb adsorption is lower than the CMC value, the number of free PS80 monomers in solution is still higher than that of FM1000 (due to FM1000's lower CMC), yet PS80 is less effective at preventing mAb adsorption. Therefore, this study shows that CMC is not the critical factor to indicate the ability to inhibit protein adsorption. As both the surfactants used in this study are chemically different, a CMC based comparison was not conducted. The second reason that FM1000 is more effective could be due to the lower surface tension than PS80 at similar mass and molar concentrations, enabling FM1000 molecules to outcompete protein adsorption onto the surface better than PS80. A higher area per molecule for FM1000 indicates that fewer FM1000 molecules are sufficient to prevent protein adsorption as opposed to PS80. This is evident from a lower surface concentration value for FM1000 as compared to PS80 for the same bulk surfactant concentration. Thus, XRR measurements along with the quantitative understanding of protein and surfactant competitive adsorption reveal molecular-level understanding of different surfactants to inhibit protein adsorption. One of the advantages of using FM1000 over PS80 would be lower levels of FM1000 concentrations in protein formulations due to its higher surface area per molecule and surface activity for a given mass and molar concentration compared to PS80, allowing FM1000 to block a larger percentage of the interfacial area. This becomes important in therapeutic formulations where it is ideal to have a minimum amount of surfactants present in the solution to prevent aggregation of proteins. A higher percentage of the surfactant itself can lead to an immune response.⁵³ Furthermore, for IV administration of drugs, it is essential to have a sufficient surfactant concentration after diluting the protein drug product to still prevent the loss of proteins upon adsorption.

Agitation Studies. Protein molecules are subjected to shaking during transportation, storage, and administration. Shaking can lead to the formation of new hydrophobic surfaces, potentially exposing protein formulation onto these fresh interfaces, increasing their adsorption and aggregation on surfaces. Other studies have shown that as proteins adsorb to the air/water interface, the interfacial stress generated from agitation leads to protein aggregation and the formation of micron-sized particles.^{50,54–58} We have compared the ability of PS80 and FM1000 to inhibit particle formation, where the population of particles as a function of surfactant excipient and surfactant concentration can serve as a downstream measure of the inhibition of protein adsorption at the interface. The rapid adsorption of surfactants to the interface should reduce protein aggregation that is an outcome of protein adsorption at the air/water interface.

As evident from our XRR measurements, surfactants above a certain concentration for a given protein concentration are

relatively able to inhibit protein adsorption onto the surface. We performed agitation shake studies with the protein concentration fixed at 2.5 mg/mL and surfactant (either PS80 or FM1000) concentrations in the range of 5.0×10^{-4} to 1.0×10^{-1} mg/mL. Figure 7 reports the particle counts (>2,

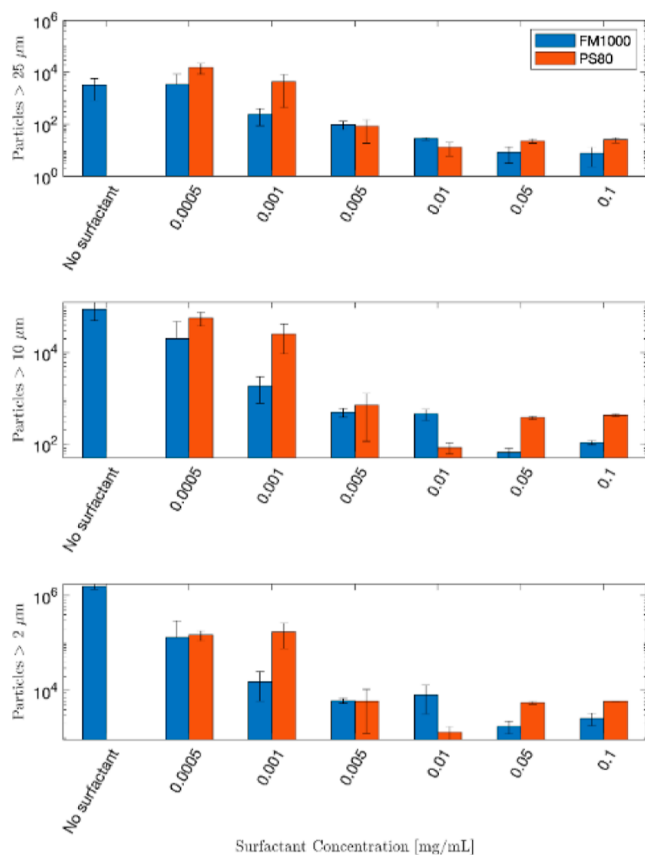


Figure 7. Particles per milliliter in mAb formulation with PS80 (red) and FM1000 (blue) after being subjected to reciprocal shaking (180 strokes/min) for 24 h at room temperature. Particles were analyzed by MFI. The error bars are the standard deviation for triplicate samples.

>10, and >25 μm) after 24 h of shaking. At the surfactant concentration range used for this study, FM1000 resulted in overall lower particle counts as compared to PS80, indicating that FM1000 is generally better able to inhibit shake-induced protein aggregation. Visual analysis of the images produced by MFI suggests that the particles are proteinaceous, as particles were predominantly aspherical and of varying translucency. For no surfactant or surfactant concentration $<5.0 \times 10^{-4}$ mg/mL, sufficient protein particle counts are detected. This correlates with our XRR measurements, which show higher levels of protein adsorption at a low surfactant concentration of PS80 compared to FM1000. For surfactant concentration of 1.0×10^{-3} mg/mL, samples with PS80 surfactants are prone to significant protein aggregation (~ 2500 particles/ml for $>10 \mu\text{m}$, and ~ 4000 particles/ml for $>25 \mu\text{m}$), while the FM1000 samples have comparatively low numbers of particles (~ 1000 particles/ml for $>10 \mu\text{m}$, and ~ 300 particles/ml for $>25 \mu\text{m}$). As the surfactant concentration is increased by 10 times (1.0×10^{-2} mg/mL), both the PS80 and FM1000 inhibit protein particle formation. Differences in absolute concentration for the surfactant required to minimize particles compared to XRR

data could be due to multiple mechanisms of aggregation and/or differences in the surface area generated by the different analysis methods.

These results are consistent with our findings from XRR measurements, where with a protein concentration of 2.5 mg/mL, surfactant concentrations greater than 1.20×10^{-2} mg/mL for PS80 and 7.86×10^{-3} mg/mL for FM1000 are sufficient to prevent the adsorption of proteins. This indicates that the minimum surfactant concentration obtained from XRR measurements can also prevent any further adsorption of proteins onto freshly created surfaces due to shaking. A further increase in the surfactant concentration for the shaking study leads to an overall lower particle count with FM1000. XRR measurements indicate that FM1000 can block a larger percentage of the surface, and therefore, during the shake studies, at a high enough FM1000 concentration, there is less protein per unit time available to form particles, leading to fewer particles in the presence of FM1000.

Adsorption on Silicone Substrates. Liquid drug formulations are often provided as prefilled syringes for self-administration by patients. Syringes are usually coated with silicone oil for ease of administration. However, mAb protein molecules can adsorb onto the silicone oil/liquid interface, promoting protein aggregation. To determine whether FM1000 or PS80 can prevent the adsorption to silicone when incubated with protein formulation, we looked at the surface fouling on a silicone substrate by measuring the contact angle. Although solid, the silicone used for this work is chemically similar to that of the silicone oil that is used to coat syringes.

Similar to the agitation studies, the protein concentration of 2.5 mg/mL is used, and the surfactant concentration is in the range of 1.0×10^{-4} to 5.0×10^{-2} mg/mL. Figure 8 reports the measured water droplet contact angle of the silicone surface following incubation with a formulation of the mAb and surfactant (FM1000 or PS80) as a function of surfactant concentration. The clean silicone surface has a contact angle of

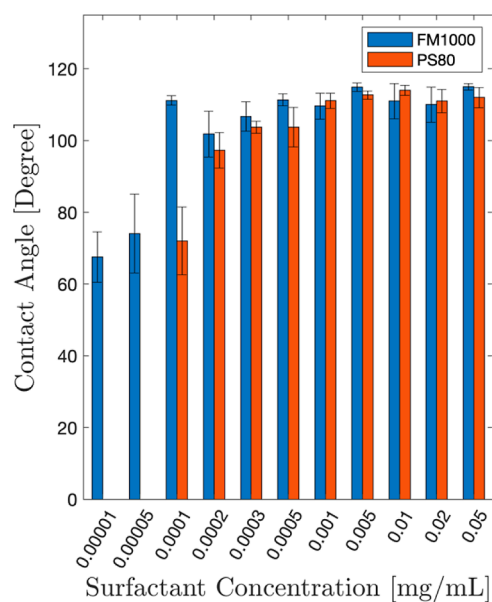


Figure 8. Water contact angle on silicone slabs following incubation of 2.5 mg/mL mAb + surfactant on the surface for 24 h. A higher contact angle indicates less fouling of the surface by the mAb.

110°. If enough surfactant molecules are present in the formulation, fouling due to mAb adsorption can be prevented, leading to contact angle maintenance of 110°. Should the mAb molecules adsorb, a decrease in contact angle measurements would be observed as the protein presents a more hydrophilic surface. The data show that FM1000 once again provides protection at lower surfactant concentrations compared to PS80 before the surface begins to foul. At a surfactant bulk concentration of 1.0×10^{-4} mg/mL, the measured contact angle in the presence of mAb protein is around 110° for FM1000 and 70° for PS80. As PS80 concentration of 1.0×10^{-4} mg/mL indicated fouling due to mAb adsorption, experiments with PS80 concentrations lower than 1.0×10^{-4} mg/mL were not performed to conserve material. As the PS80 concentration is increased by 10 times to 1.0×10^{-3} mg/mL, the contact angle increases to 110°, indicating that mAb adsorption is inhibited. The surfactant concentration required to prevent surface fouling for both FM1000 and PS80 is different than that from the agitation or XRR studies. One of the possible reasons is that the mechanism of surfactant adsorption is different on an air/water interface compared to a silicone/water interface. These surface studies also measure irreversible adsorption, while our XRR studies do not probe the reversibility of the adsorbed layer. Similarly, our agitation studies only probe the downstream effect of adsorption-sub-visible particles—but the pathway to aggregation through the interface is not probed. Future studies will be focused on the understanding of protein-FM1000 interactions at a silicone/liquid interface.

CONCLUSIONS

In this work, we explored the molecular-level understanding of FM1000 and PS80 excipients for the stability of a mAb-based protein formulation upon interfacial adsorption. We found that FM1000 has a lower surface tension than PS80 at similar mass and molar concentrations, and therefore, FM1000 adsorbs faster onto the air/water interface. Additionally, the pendant bubble tensiometer and XRR measurements for the surfactant alone system showed a higher area per molecule for adsorbed FM1000 than PS80 molecules. This indicates that fewer FM1000 molecules are sufficient to saturate the air/water interface and can therefore prevent the adsorption of protein molecules at lower concentrations of excipient. In order to inhibit mAb adsorption at the air/water interface with an increase in mAb bulk concentration, FM1000 concentration of 7.86×10^{-3} mg/mL was sufficient. On the other hand, for the highest mAb concentration of 2.5 mg/mL used in this study, four times higher PS80 concentration relative to FM1000 was required to block mAbs from adsorbing to the surface. Additionally, agitation and surface-fouling studies correlated well with the XRR measurements. Overall, this study suggests that the design of new excipients, such as FM1000, should focus on high interfacial footprints to effectively compete for interfacial area with mAbs and other proteins.

ASSOCIATED CONTENT

Supporting Information

The Supporting Information is available free of charge at <https://pubs.acs.org/doi/10.1021/acs.molpharmaceut.2c00152>.

Langmuir adsorption isotherm fit to determine cmc and maximum surface coverage for PS80 and FM1000; X-ray

reflectivity data analysis; surface concentration calculations for single component (mAb or PS80 or FM1000) and mixed component (mAb + PS80 or mAb + FM1000); homology modeling along with the estimate for mAb size; XRR profile with the corresponding EDP for pure PS80, pure FM1000, mAb + PS80, and mAb + FM1000; and overlapping XRR measurements to compare the mixed component system alongside the pure mAb and pure surfactant XRR data (PDF)

AUTHOR INFORMATION

Corresponding Authors

Ankit D. Kanthe — Sterile Product Development, Bristol Myers Squibb, New Brunswick, New Jersey 08901, United States; Department of Chemical Engineering, The City College of New York, New York, New York 10031, United States; orcid.org/0000-0003-4451-5383; Email: Ankit.Kanthe@bms.com

Raymond S. Tu — Department of Chemical Engineering, The City College of New York, New York, New York 10031, United States; orcid.org/0000-0002-6192-7665; Email: tu@ccny.cuny.edu

Authors

Miriam R. Carnovale — Pharma Solutions R&D, International Flavors and Fragrances, Wilmington, Delaware 19803, United States

Joshua S. Katz — Pharma Solutions R&D, International Flavors and Fragrances, Wilmington, Delaware 19803, United States; orcid.org/0000-0002-0046-4062

Susan Jordan — Pharma Solutions R&D, International Flavors and Fragrances, Wilmington, Delaware 19803, United States

Mary E. Krause — Sterile Product Development, Bristol Myers Squibb, New Brunswick, New Jersey 08901, United States; orcid.org/0000-0002-3299-5423

Songyan Zheng — Sterile Product Development, Bristol Myers Squibb, New Brunswick, New Jersey 08901, United States

Andrew Ilott — Sterile Product Development, Bristol Myers Squibb, New Brunswick, New Jersey 08901, United States

William Ying — Sterile Product Development, Bristol Myers Squibb, New Brunswick, New Jersey 08901, United States

Wei Bu — NSF's ChemMatCARS, Center for Advanced Radiation Sources, University of Chicago, Chicago, Illinois 606371, United States; orcid.org/0000-0002-9996-3733

Mrinal K. Bera — NSF's ChemMatCARS, Center for Advanced Radiation Sources, University of Chicago, Chicago, Illinois 606371, United States; orcid.org/0000-0003-0698-5253

Binhua Lin — NSF's ChemMatCARS, Center for Advanced Radiation Sources, University of Chicago, Chicago, Illinois 606371, United States; orcid.org/0000-0001-5932-4905

Charles Maldarelli — Department of Chemical Engineering and Levich Institute, The City College of New York, New York, New York 10031, United States; orcid.org/0000-0001-7427-2349

Complete contact information is available at: <https://pubs.acs.org/doi/10.1021/acs.molpharmaceut.2c00152>

Notes

The authors declare no competing financial interest.

ACKNOWLEDGMENTS

We acknowledge the financial support from Bristol–Myers Squibb Co. R.S.T. and A.D.K. thank the support of the National Science Foundation under Grant no. 1605904. J.S.K thanks Ben Yezer, Hadi Fares, and Abigail Nolin for help in development of the contact angle method. For this research, XRR measurements were conducted at NSF's ChemMatCARS Sector 15 that is principally supported by the Divisions of Chemistry (CHE) and Materials Research (DMR), National Science Foundation (NSF), under grant number NSF/CHE-1834750. Use of the Advanced Photon Source (APS), an Office of Science User Facility operated for the U.S. Department of Energy (DOE) Office of Science by Argonne National Laboratory (ANL), was supported by the U.S. DOE under Contract no. DE-AC02-06CH11357.

REFERENCES

- (1) Zhang, Q.; Chen, G.; Liu, X.; Qian, Q. Monoclonal Antibodies as Therapeutic Agents in Oncology and Antibody Gene Therapy. *Cell Res.* **2007**, *17*, 89–99.
- (2) Mitragotri, S.; Burke, P. A.; Langer, R. Overcoming the Challenges in Administering Biopharmaceuticals: Formulation and Delivery Strategies. *Nat. Rev. Drug Discovery* **2014**, *13*, 655–672.
- (3) Kanthe, A. D.; Maldarelli, C.; Tu, R. Interfacial Behaviors of Proteins. In *Protein Instability at Interfaces During Drug Product Development*; Li, J., Krause, M. E., Tu, R., Eds.; AAPS Advances in the Pharmaceutical Sciences Series; Springer International Publishing: Cham, 2021; Vol. 43, pp 51–114.
- (4) Kanthe, A. D.; Tu, R.; Maldarelli, C. Protein Adsorption at a Gas-Aqueous Interface. In *Protein Instability at Interfaces During Drug Product Development*; Li, J., Krause, M. E., Tu, R., Eds.; AAPS Advances in the Pharmaceutical Sciences Series; Springer International Publishing: Cham, 2021; Vol. 43, pp 9–49.
- (5) McClellan, S. J.; Franses, E. I. Effect of Concentration and Denaturation on Adsorption and Surface Tension of Bovine Serum Albumin. *Colloids Surf., B* **2003**, *28*, 63–75.
- (6) Wang, L.; Cai, P.; Galla, H.-J.; He, H.; Flach, C. R.; Mendelsohn, R. Monolayer-Multilayer Transitions in a Lung Surfactant Model: IR Reflection-Absorption Spectroscopy and Atomic Force Microscopy. *Eur. Biophys. J.* **2005**, *34*, 243–254.
- (7) Smith, C.; Li, Z.; Holman, R.; Pan, F.; Campbell, R. A.; Campana, M.; Li, P.; Webster, J. R. P.; Bishop, S.; Narwal, R.; Uddin, S.; van der Walle, C. F.; Lu, J. R. Antibody Adsorption on the Surface of Water Studied by Neutron Reflection. *mAbs* **2017**, *9*, 466–475.
- (8) Dixit, N.; Maloney, K. M.; Kalonia, D. S. Protein-Silicone Oil Interactions: Comparative Effect of Nonionic Surfactants on the Interfacial Behavior of a Fusion Protein. *Pharm. Res.* **2013**, *30*, 1848–1859.
- (9) Vargo, K. B.; Stahl, P.; Hwang, B.; Hwang, E.; Giordano, D.; Randolph, P.; Celentano, C.; Hepler, R.; Amin, K. Surfactant Impact on Interfacial Protein Aggregation and Utilization of Surface Tension to Predict Surfactant Requirements for Biological Formulations. *Mol. Pharm.* **2021**, *18*, 148–157.
- (10) Serno, T.; Härtl, E.; Besheer, A.; Miller, R.; Winter, G. The Role of Polysorbate 80 and HP β CD at the Air-Water Interface of IgG Solutions. *Pharm. Res.* **2013**, *30*, 117.
- (11) Kannan, A.; Shieh, I. C.; Fuller, G. G. Linking Aggregation and Interfacial Properties in Monoclonal Antibody-Surfactant Formulations. *J. Colloid Interface Sci.* **2019**, *550*, 128–138.
- (12) Tein, Y. S.; Zhang, Z.; Wagner, N. J. Competitive Surface Activity of Monoclonal Antibodies and Nonionic Surfactants at the Air-Water Interface Determined by Interfacial Rheology and Neutron Reflectometry. *Langmuir* **2020**, *36*, 7814–7823.
- (13) Shieh, I. C.; Patel, A. R. Predicting the Agitation-Induced Aggregation of Monoclonal Antibodies Using Surface Tensiometry. *Mol. Pharm.* **2015**, *12*, 3184–3193.
- (14) Roberts, C. J. Therapeutic Protein Aggregation: Mechanisms, Design, and Control. *Trends Biotechnol.* **2014**, *32*, 372–380.
- (15) Yano, Y. F.; Uruga, T.; Tanida, H.; Toyokawa, H.; Terada, Y.; Takagaki, M.; Yamada, H. Driving Force Behind Adsorption-Induced Protein Unfolding: A Time-Resolved X-Ray Reflectivity Study on Lysozyme Adsorbed at an Air / Water Interface. *Langmuir* **2009**, *25*, 32–35.
- (16) Leiske, D. L.; Shieh, I. C.; Tse, M. L. A Method to Measure Protein Unfolding at an Air-Liquid Interface. *Langmuir* **2016**, *32*, 9930–9937.
- (17) Carpenter, J.; Cherney, B.; Lubinecki, A.; Ma, S.; Marszal, E.; Mire-Sluis, A.; Nikolai, T.; Novak, J.; Ragheb, J.; Simak, J. Meeting Report on Protein Particles and Immunogenicity of Therapeutic Proteins: Filling in the Gaps in Risk Evaluation and Mitigation. *Biologics* **2010**, *38*, 602–611.
- (18) Wang, W.; Nema, S.; Teagarden, D. Protein Aggregation-Pathways and Influencing Factors. *Int. J. Pharm.* **2010**, *390*, 89–99.
- (19) Wang, W. Protein Aggregation and Its Inhibition in Biopharmaceutics. *Int. J. Pharm.* **2005**, *289*, 1–30.
- (20) Ohtake, S.; Kita, Y.; Arakawa, T. Interactions of Formulation Excipients with Proteins in Solution and in the Dried State. *Adv. Drug Delivery Rev.* **2011**, *63*, 1053–1073.
- (21) Frokjaer, S.; Otzen, D. E. Protein Drug Stability: A Formulation Challenge. *Nat. Rev. Drug Discovery* **2005**, *4*, 298–306.
- (22) Den Engelsman, J.; Garidel, P.; Smulders, R.; Koll, H.; Smith, B.; Bassarab, S.; Seidl, A.; Hainzl, O.; Jiskoot, W. Strategies for the Assessment of Protein Aggregates in Pharmaceutical Biotech Product Development. *Pharm. Res.* **2011**, *28*, 920–933.
- (23) Wang, W. Instability, Stabilization, and Formulation of Liquid Protein Pharmaceuticals. *Int. J. Pharm.* **1999**, *185*, 129–188.
- (24) Kamerzell, T. J.; Esfandiary, R.; Joshi, S. B.; Middaugh, C. R.; Volkin, D. B. Protein-Excipient Interactions: Mechanisms and Biophysical Characterization Applied to Protein Formulation Development. *Adv. Drug Delivery Rev.* **2011**, *63*, 1118–1159.
- (25) Kumar, R. Role of Naturally Occurring Osmolytes in Protein Folding and Stability. *Arch. Biochem. Biophys.* **2009**, *491*, 1–6.
- (26) Jordan, S.; Katz, J. S.; Yezer, B. Excipients: Characterization, Purpose, and Selection. In *Protein Instability at Interfaces During Drug Product Development*; Li, J., Krause, M. E., Tu, R., Eds.; AAPS Advances in the Pharmaceutical Sciences Series; Springer International Publishing: Cham, 2021; Vol. 43, pp 249–269.
- (27) Mahler, H.-C.; Senner, F.; Maeder, K.; Mueller, R. Surface Activity of a Monoclonal Antibody. *J. Pharm. Sci.* **2009**, *98*, 4525–4533.
- (28) Patapoff, T. W.; Esue, O. Polysorbate 20 Prevents the Precipitation of a Monoclonal Antibody during Shear. *Pharm. Dev. Technol.* **2009**, *14*, 659–664.
- (29) Lee, H. J.; McAuley, A.; Schilke, K. F.; McGuire, J. Molecular Origins of Surfactant-Mediated Stabilization of Protein Drugs. *Adv. Drug Delivery Rev.* **2011**, *63*, 1160–1171.
- (30) Katakam, M.; Banga, A. K. Use of Poloxamer Polymers to Stabilize Recombinant Human Growth Hormone Against Various Processing Stresses. *Pharm. Dev. Technol.* **1997**, *2*, 143–149.
- (31) Kim, H. L.; McAuley, A.; Livesay, B.; Gray, W. D.; McGuire, J. Modulation of Protein Adsorption by Poloxamer 188 in Relation to Polysorbates 80 and 20 at Solid Surfaces. *J. Pharm. Sci.* **2014**, *103*, 1043–1049.
- (32) Katz, J. S.; Chou, D. K.; Christian, T. R.; Das, T. K.; Patel, M.; Singh, S. N.; Wen, Y. Emerging Challenges and Innovations in Surfactant-Mediated Stabilization of Biologic Formulations. *J. Pharm. Sci.* **2022**, *111*, 919–932.
- (33) Labrenz, S. R. Ester Hydrolysis of Polysorbate 80 in MAb Drug Product: Evidence in Support of the Hypothesized Risk after the Observation of Visible Particulate in MAb Formulations. *J. Pharm. Sci.* **2014**, *103*, 2268–2277.
- (34) Dwivedi, M.; Blech, M.; Presser, I.; Garidel, P. Polysorbate Degradation in Biotherapeutic Formulations: Identification and Discussion of Current Root Causes. *Int. J. Pharm.* **2018**, *552*, 422–436.

- (35) Kishore, R. S. K.; Kiese, S.; Fischer, S.; Pappenberger, A.; Grauschopf, U.; Mahler, H.-C. The Degradation of Polysorbates 20 and 80 and Its Potential Impact on the Stability of Biotherapeutics. *Pharm. Res.* **2011**, *28*, 1194–1210.
- (36) Siska, C. C.; Pierini, C. J.; Lau, H. R.; Latypov, R. F.; Matthew Fesinmeyer, R.; Litowsk, J. R. Free Fatty Acid Particles in Protein Formulations, Part 2: Contribution of Polysorbate Raw Material. *J. Pharm. Sci.* **2015**, *104*, 447–456.
- (37) Doshi, N.; Giddings, J.; Luis, L.; Wu, A.; Ritchie, K.; Liu, W.; Chan, W.; Taing, R.; Chu, J.; Sreedhara, A.; Kannan, A.; Kei, P.; Shieh, I.; Graf, T.; Hu, M. A Comprehensive Assessment of All-Oleate Polysorbate 80: Free Fatty Acid Particle Formation, Interfacial Protection and Oxidative Degradation. *Pharm. Res.* **2021**, *38*, 531–548.
- (38) Doshi, N.; Martin, J.; Tomlinson, A. Improving Prediction of Free Fatty Acid Particle Formation in Biopharmaceutical Drug Products: Incorporating Ester Distribution during Polysorbate 20 Degradation. *Mol. Pharm.* **2020**, *17*, 4354–4363.
- (39) Bates, T. R.; Nightingale, C. H.; Dixon, E. Kinetics of Hydrolysis of Polyoxyethylene (20) Sorbitan Fatty Acid Ester Surfactants. *J. Pharm. Pharmacol.* **2011**, *25*, 470–477.
- (40) Vaclaw, C.; Merritt, K.; Pringle, V.; Whitaker, N.; Gokhale, M.; Carvalho, T.; Pan, D.; Liu, Z.; Bindra, D.; Khossravi, M.; Bolgar, M.; Volkin, D. B.; Ogunyankin, M. O.; Dhar, P. Impact of Polysorbate 80 Grade on the Interfacial Properties and Interfacial Stress Induced Subvisible Particle Formation in Monoclonal Antibodies. *J. Pharm. Sci.* **2021**, *110*, 746–759.
- (41) Khan, T. A.; Mahler, H.-C.; Kishore, R. S. K. Key Interactions of Surfactants in Therapeutic Protein Formulations: A Review. *Eur. J. Pharm. Biopharm.* **2015**, *97*, 60–67.
- (42) Katz, J. S.; Nolin, A.; Yezer, B. A.; Jordan, S. Dynamic Properties of Novel Excipient Suggest Mechanism for Improved Performance in Liquid Stabilization of Protein Biologics. *Mol. Pharm.* **2019**, *16*, 282–291.
- (43) Hanson, M. G.; Katz, J. S.; Ma, H.; Putterman, M.; Yezer, B. A.; Petermann, O.; Reineke, T. M. Effects of Hydrophobic Tail Length Variation on Surfactant-Mediated Protein Stabilization. *Mol. Pharm.* **2020**, *17*, 4302–4311.
- (44) Katz, J. S.; Tan, Y.; Kuppanan, K.; Song, Y.; Brennan, D. J.; Young, T.; Yao, L.; Jordan, S. Amino-Acid-Incorporating Nonionic Surfactants for Stabilization of Protein Pharmaceuticals. *ACS Biomater. Sci. Eng.* **2016**, *2*, 1093–1096.
- (45) Kanthe, A. D.; Krause, M.; Zheng, S.; Ilott, A.; Li, J.; Bu, W.; Bera, M. K.; Lin, B.; Maldarelli, C.; Tu, R. S. Armoring the Interface with Surfactants to Prevent the Adsorption of Monoclonal Antibodies. *ACS Appl. Mater. Interfaces* **2020**, *12*, 9977–9988.
- (46) Lin, B.; Meron, M.; Gebhardt, J.; Graber, T.; Schlossman, M. L.; Viccaro, P. J. The Liquid Surface/Interface Spectrometer at ChemMatCARS Synchrotron Facility at the Advanced Photon Source. *Phys. B* **2003**, *336*, 75–80.
- (47) Schlossman, M. L.; Synal, D.; Guan, Y.; Meron, M.; Shea-McCarthy, G.; Huang, Z.; Acero, A.; Williams, S. M.; Rice, S. A.; Viccaro, P. J. A Synchrotron X-Ray Liquid Surface Spectrometer. *Rev. Sci. Instrum.* **1997**, *68*, 4372–4384.
- (48) Pershan, P. S.; Schlossman, M. L. *Liquid Surfaces and Interfaces: Synchrotron X-Ray Methods*; Cambridge University Press: Cambridge, 2012.
- (49) Zheng, S.; Adams, M.; Mantri, R. V. An Approach to Mitigate Particle Formation on the Dilution of a Monoclonal Antibody Drug Product in an IV Administration Fluid. *J. Pharm. Sci.* **2016**, *105*, 1349–1350.
- (50) Li, J.; Krause, M. E.; Chen, X.; Cheng, Y.; Dai, W.; Hill, J. J.; Huang, M.; Jordan, S.; LaCasse, D.; Narhi, L.; Shalae, E.; Shieh, I. C.; Thomas, J. C.; Tu, R.; Zheng, S.; Zhu, L. Interfacial Stress in the Development of Biologics: Fundamental Understanding, Current Practice, and Future Perspective. *AAPS J.* **2019**, *21*, 44.
- (51) Miller, R.; Aksenenko, E. V.; Fainerman, V. B.; Pison, U. Kinetics of Adsorption of Globular Proteins at Liquid/Fluid Interfaces. *Colloids Surf., A* **2001**, *183–185*, 381–390.
- (52) Kanthe, A.; Ilott, A.; Krause, M.; Zheng, S.; Li, J.; Bu, W.; Bera, M. K.; Lin, B.; Maldarelli, C.; Tu, R. S. No Ordinary Proteins: Adsorption and Molecular Orientation of Monoclonal Antibodies. *Sci. Adv.* **2021**, *7*, No. eabg2873.
- (53) Hermeling, S.; Schellekens, H.; Crommelin, D. J. A.; Jiskoot, W. Micelle-Associated Protein in Epoetin Formulations: A Risk Factor for Immunogenicity? *Pharm. Res.* **2003**, *20*, 1903–1907.
- (54) Krause, M. E.; Zheng, S.; Shieh, I. C.; Ogunyankin, M. O. Evaluation of Interfacial Stress During Drug Product Development. In *Protein Instability at Interfaces During Drug Product Development*; Li, J., Krause, M. E., Tu, R., Eds.; Springer International Publishing: Cham, 2021; pp 131–152.
- (55) Lin, G. L.; Pathak, J. A.; Kim, D. H.; Carlson, M.; Riguero, V.; Kim, Y. J.; Buff, J. S.; Fuller, G. G. Interfacial Dilatational Deformation Accelerates Particle Formation in Monoclonal Antibody Solutions. *Soft Matter* **2016**, *12*, 3293–3302.
- (56) Koepf, E.; Eisele, S.; Schroeder, R.; Brezesinski, G.; Friess, W. Notorious but Not Understood: How Liquid-Air Interfacial Stress Triggers Protein Aggregation. *Int. J. Pharm.* **2018**, *537*, 202–212.
- (57) Sorret, L. L.; DeWinter, M. A.; Schwartz, D. K.; Randolph, T. W. Protein-Protein Interactions Controlling Interfacial Aggregation of RhIL-1ra Are Not Described by Simple Colloid Models. *Protein Sci.* **2018**, *27*, 1191–1204.
- (58) Ogunyankin, M. O.; Deshmukh, S.; Krause, M. E.; Carvalho, T.; Huang, M.; Ilott, A.; Remy, B.; Khossravi, M. Small-Scale Tools to Assess the Impact of Interfacial and Shear Stress on Biologic Drug Products. *AAPS PharmSciTech* **2019**, *20*, 184.

Recommended by ACS

Investigating the Orientation of an Interfacially Adsorbed Monoclonal Antibody and Its Fragments Using Neutron Reflection

Sean Ruane, Jian R. Lu, *et al.*

FEBRUARY 16, 2023

MOLECULAR PHARMACEUTICS

READ 

Probing Molecular Interactions of Antibody Drugs, Silicone Oil, and Surfactant at Buried Interfaces In Situ

Tieyi Lu, Zhan Chen, *et al.*

OCTOBER 10, 2022

ANALYTICAL CHEMISTRY

READ 

Novel HER2-Targeted Peptide for NIR-II Imaging of Tumor

Rui Cao, Zhen Cheng, *et al.*

JANUARY 20, 2023

MOLECULAR PHARMACEUTICS

READ 

Voices in *Molecular Pharmaceutics*: Meet Darnell Cuylear, Who Combines Dentistry and Science to Design Calcium Phosphate Delivery Systems for Enhanced Tooth Stability

Darnell Cuylear.

FEBRUARY 02, 2023

MOLECULAR PHARMACEUTICS

READ 

Get More Suggestions >